# Compensation for Non-stationary Detector Response in Analytical Varying Focal-length Fan-beam SPECT Reconstruction

Tianfang Li, *Student Member, IEEE*, Junhai Wen, *Member, IEEE,* and Zhengrong Liang, *Member, IEEE*

*Abstract* — **In this study, a non-stationary filtering technique was developed to compensate for spatially variant detector response in varying focal-length fan-beam (VFF) collimated SPECT. First a collimator coordinate system was introduced in order to derive the geometric transfer function and the frequency-distance relation for VFF collimator from its parallel-beam and fan-beam counterparts, and then the Fourier transform of the detector response was computed and used to construct a Wiener filter. The filter was applied to the blurred projection data before image reconstruction. Experimental results demonstrated improved resolution in reconstructed images after the non-stationary filtering.**

## I. Introduction

IT is well known that the spatially varying focal-length fan-beam (VFF) collimation has the advantages of improving sensitivity and resolution, while avoiding the truncation problem in SPECT (single photon emission computed tomography), and has the potential for clinical use in chest studies. However, due to the relatively complicate geometry, there are only iterative ways for the image reconstruction of VFF collimated SPECT with consideration of both non-uniform attenuation and collimator blurring effects to date [1]. Since the discovery of inversion formula for non-uniformly attenuated Radon transform recently by Novikov, *et al.* [2, 3], a completely analytical reconstruction framework for parallel-beam SPECT has been established with simultaneous consideration of Poisson noise, Compton scatter, non-uniform attenuation and non-stationary detector response [4], and the reconstruction problems for non-parallel geometries were also investigated. It has been shown that an analytical reconstruction method exists for both fan-beam and VFF geometries with compensation for the non-uniform attenuation [5, 6]. In this work, our efforts are focused on the compensation for the non-stationary detector response in VFF geometry analytically, so that a complete non-iterative reconstruction framework for VFF collimated SPECT can be established.

Manuscript submitted on November 12, 2002. This work was supported in part by the NIH National Heart, Lung and Blood Institute under Grant No. HL54166.

T. Li is with the Departments of Physics and Astronomy and Radiology. State University of New York, Stony Brook, NY 11790 USA (telephone: 631-444-7999, e-mail: tfli@clio.rad.sunysb.edu).

J. Wen is with the Department of Radiology, State University of New York, Stony Brook, NY 11794, USA.

Z. Liang is with the Departments of Radiology and Computer Science, State University of New York, Stony Brook, NY 11794, USA.

The spatially variant detector response was studied by Metz and Tsui *et al.* for parallel-, fan- and cone-beam geometries [7, 8]. It has been shown that both distance dependent and shift invariant properties may exist for these geometries under certain coordinate systems [9]. To compensate for the detector response, a filtering technique had been proposed by Edholm, Hawkins, Lewitt, and Glick *et al.* for parallel-beam geometry based on the frequency-distance relation (FDR) on circular orbit [10-14]. Later Ye, *et al.* extended the filtering technique to non-circular orbit SPECT [15] and Cao, *et al.* developed the filters for fan-beam and cone-beam geometries [16].

In this paper, we further extended the filtering technique to VFF geometry. Unlike the fan-beam geometry, the geometric transfer function (GTF) for VFF collimators cannot be expressed as shift invariant in the collimator coordinate space for any fixed distance, which makes the extension very challenging. Therefore we proposed a reasonable approximation and developed a non-stationary filter to mitigate this problem. In the following sections, we first introduce a collimator coordinate system (CCS), under which the GTF for VFF geometry is presented, and then the FDR is derived for VFF geometry. In implementing our filter, we adapt the fan-beam strategy [16] with a reasonable approximation to simplify the problem for an improved filtering for VFF geometry.

In our preliminary phantom simulation studies, the developed VFF filter was applied to blurred projection data first, and then the deblurred data was reconstructed using our analytical method with non-uniform attenuation compensation [5, 6]. Noticeable improvement in the reconstructed images was seen after the filtering. We further discussed the approximation in this method as well as in fan-beam and cone-beam geometries.

## II. Theory

Described below are the CCS, the GTF and the FDR for VFF geometry. The formulas for parallel-beam and fan-beam geometries are also presented for comparison purpose.

### A. Collimator Coordinate System

To develop the GTF and FDR for any detector system, we introduce a general "collimator coordinate system" or the CCS of $\xi - \eta$ as shown in Figure 1, restricted to one slice for simplicity. The CCS is detailed as follows: any point in this coordinate system is represented by $(\xi, \eta)$, where $\xi$ is defined as the location on the detection plane

where the point is being projected; and $\eta$ is the distance from the point to the detection plane. More precisely, the focal point, the source point, and the detection point lie in one straight line.

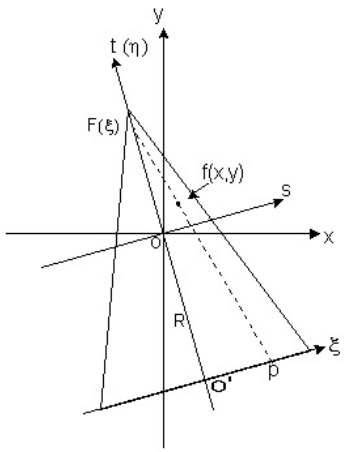


Fig. 1. Collimator coordinate system and other coordinate systems.

The relationships among the coordinate systems in Figure 1 are:

$$(x, y) = (\rho\cos\varphi, \rho\sin\varphi), \quad (1)$$

$$(s, t) = (x\cos\theta + y\sin\theta, -x\sin\theta + y\cos\theta), \quad (2)$$

$$(\xi, \eta) = (\frac{sf(\xi)}{f(\xi) - R - t}, R + t). \quad (3)$$

### *B. Geometric Transfer Function for VFF Collimators*

The above CCS has the advantage that the GTFs for parallel-, fan-, and cone-beam geometries have the shift invariant property [9].

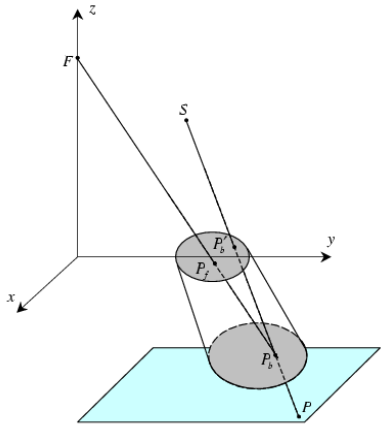


Fig. 2. Geometrical model for the point-spread function of varying focal-length fan-beam collimators.

Using the geometric model as shown in Figure 2, and following the derivation of Metz and Tsui *et al.* [7,8], we can derive the GTF for VFF geometry in terms of the integral of the aperture function (using the same definition and notation, as in [7,8]):

$$\phi_{VFF}(\mathbf{r_0}, \mathbf{r}) = \mathbf{K}\iint a(-\boldsymbol{\sigma})a(\mathbf{r_T} - \boldsymbol{\sigma})d^2\sigma \quad (4)$$

where

$$\mathbf{K} = \frac{z_0 + L + B}{4\pi A\left[(z_0 + L + B)^2 + (x - x_0)^2 + (y - y_0)^2\right]^{3/2}} \quad (5)$$

and

$$r_{Tx} = \frac{L}{Z + L + B}(x - x_0) \quad (6)$$

$$r_{Ty} = \frac{L}{Z + L + B}[\frac{F - Z}{F + L}y - \frac{F + L + B}{F + L}y_0] \quad (7)$$

where the focal length $F$ in eqn. (7) is the function of $y$, i.e. $F = F(y)$. Note that if the focal length $F$ is a constant, eqn. (4) becomes the function for fan-beam geometry.

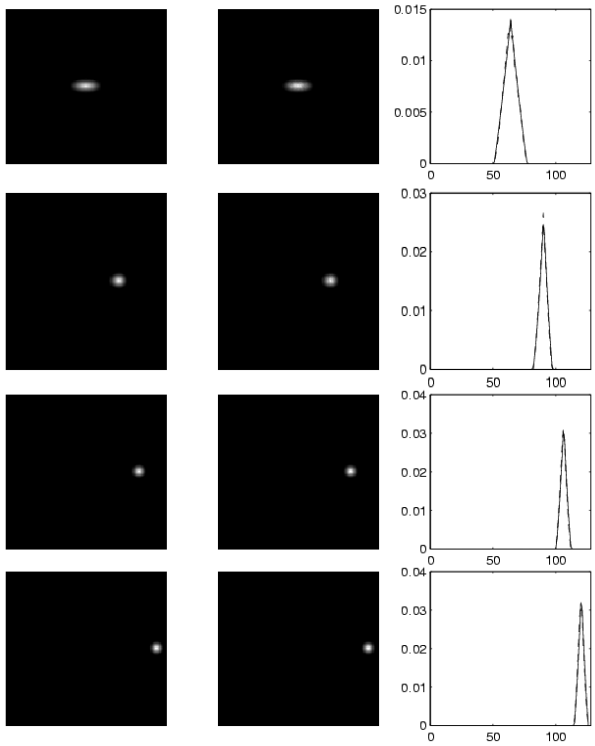


Fig. 3. Comparison of calculated geometrical PSF (left column) with Monte-Carlo simulation (middle column) at depth 35cm and offset of 0, 5, 10, 15 cm respectively (from top to bottom). The right column shows the profiles through the center, with the calculated geometrical PSF in solid line and the simulation in dashed line.

When the above CCS is applied, we have

$$(x_0, y_0) = (x_{0C}, y_{0C} = \frac{F + L + B}{F - Z}y_0) \quad (8)$$

and

$$r_y = \frac{L}{Z + L + B}[\frac{F - Z}{F + L}(y - y_{0C})] \quad (9)$$

where parallel- or fan-beam GTF can be expressed as:

$$\phi_F(\boldsymbol{r}_{0C}, \boldsymbol{r}) = \phi(x - x_{0C}, y - y_{0C}, z_0) \quad (10)$$

which reflects the shift invariant property of parallel- or fan-beam collimator at any plane at a fixed distance $z_0$ to the collimator surface. However, for VFF geometry, this shift invariant property no longer exists. Under the CCS, the GTF of VFF collimator can only be written as:

$$\phi_{VFF} = \phi(x - x_{0C}, y - y_{0C}, y_{0C}, z_0) \quad (11)$$

In Figure 3 above, we compared the Monte-Carlo simulation results with our calculated geometric point-spread functions (PSFs). The shift variance is seen.

### C. Frequency Distance Relation for VFF Geometry

The 2D Fourier transform (FT) $P(n,\omega)$ of a sinogram of projection data $p(\theta,\xi)$ is given by

$$P(n,\omega)=\int_0^{2\pi} d\theta \int_{-\infty}^{\infty} d\xi e^{-2\pi i(n\theta+\omega\xi)} p(\theta,\xi) \tag{12}$$

where $n$ and $\omega$ are the angular frequency (corresponding to the projection angle $\theta$) and spatial frequency (corresponding to the position on the detector $\xi$), respectively. The complex exponential in the integrand of eqn. (12) can be interpreted as a 2D plane wave in the $n$-$\omega$ plane [10], and its phase $n\theta+\omega\xi$ and amplitude $p(\theta,\xi)$ depend on $\theta$ and $\xi$. The plane wave is a fast oscillating function of $\theta$ and $\xi$, so the integration of (12) is approximately zero except for $n\theta+\omega\xi=c+2k\pi$ where $c$ is a constant and $k$ is an integer. We take derivative with respect to $\theta$ on both sides, as $n$ and $\omega$ do not depend on $\theta$, we have

$$\frac{d\xi}{d\theta}=-\frac{n}{\omega} \tag{13}$$

This equation originally derived from the parallel-beam geometry is still true for VFF geometry. And from eqns. (1), (2), and (3) we have

$$\frac{d\xi}{d\theta}=\frac{F^2(\eta-R)-\xi^2(F-\eta)}{F(F-\eta)+\xi\eta F'} \tag{14}$$

where $F'$ denotes derivative of focal length function $F(\xi)$ with respect to $\xi$. The FDR for VFF geometry is obtained using eqns. (13) and (14):

$$P(n,\omega)\neq 0 \quad \text{for} \quad \frac{n}{\omega}=\frac{\xi^2(F-\eta)-F^2(\eta-R)}{F(F-\eta)+\xi\eta F'} \tag{15}$$

or rewritten as

$$\eta=\frac{nF^2-\omega F(FR+\xi^2)}{n(F-F'\xi)-\omega(F^2+\xi^2)}=u(n,\omega,\xi) \tag{16}$$

Note that when $F(\xi)$ = constant, $F'=0$, the VFF becomes fan-beam geometry and eqn. (16) becomes

$$\eta=\frac{nF^2-F\omega(FR+\xi^2)}{nF-\omega(F^2+\xi^2)}=u(n,\omega,\xi) \tag{17}$$

When $F\to\infty$, it becomes parallel-beam geometry, and

$$\eta=-\frac{n}{\omega}+R=u(n,\omega)\,. \tag{18}$$

where the independence on $\xi$ for parallel-beam is seen, but not for fan-beam and VFF geometries.

## III. Review of Filter in Parallel-beam and Fan-beam Geometries

The FDR can be used to derive a filtering technique to compensate for the distance-dependent detector response in image reconstruction.

### A. Derivation of Filter for Parallel-beam Collimator

For parallel-beam, the ideal projection and its 3D FT are:

$$p(\theta,\xi,z)=\int_{-\infty}^{\infty} f(\theta;\xi,\eta,z)d\eta$$

$$\begin{aligned}P(n,\omega_\xi,\omega_z)&=\int_0^{2\pi} d\theta e^{-2\pi in\theta}\int_{-\infty}^{\infty} d\xi e^{-2\pi i\omega_\xi\xi}\\&\quad\times\int_{-\infty}^{\infty} dz e^{-2\pi i\omega_z z}\int_{-\infty}^{\infty} d\eta f(\theta;\xi,\eta)\\&=\int_0^{2\pi} d\theta e^{-2\pi in\theta}\int_{-\infty}^{\infty} d\xi e^{-2\pi i\omega_\xi\xi}\int_{-\infty}^{\infty} dz e^{-2\pi i\omega_z z} f(\theta;\xi,u)\end{aligned} \tag{19}$$

where the measured blurred projection data and its 3D FT are:

$$\begin{aligned}p^b(\theta,\xi,z)&=\int_{-\infty}^{\infty} d\xi'\int_{-\infty}^{\infty} d\eta'\\&\quad\times\int_{-\infty}^{\infty} dz' f(\theta;\xi',\eta',z')h(\xi-\xi',z-z',\eta')\\P^b(n,\omega_\xi,\omega_z)&=\int_0^{2\pi} d\theta e^{-2\pi in\theta}\int_{-\infty}^{\infty} d\xi' e^{-2\pi i\omega_\xi\xi'}\int_{-\infty}^{\infty} dz' e^{-2\pi i\omega_z z'} f(\theta;\xi',u)\\&\quad\times H(\omega_\xi,\omega_z,-n/\omega_\xi+R)\end{aligned} \tag{20}$$

where the FDR for parallel-beam geometry of eqn. (18) has been adopted in the above derivation. From eqns. (19) and (20) it is clear that

$$P(n,\omega_\xi,\omega_z)=P^b(n,\omega_\xi,\omega_z)H^{-1}(\omega_\xi,\omega_z,-n/\omega_\xi+R) \tag{21}$$

### B. Derivation of Filter for Fan-beam Geometry

The geometric model indicates that the PSF for fan-beam geometry is shift invariant for fixed distance under the CCS. Therefore, the collimator blurred projection data can still be expressed as the convolution of the object with the PSF. However, the integral under fan-beam CCS has another term known as the Jacobian factor. The blurred projection data is

$$\begin{aligned}p^b(\theta,\xi,z)&=\int_{-\infty}^{\infty} d\xi'\int_{-\infty}^{\infty} d\eta'\\&\quad\times\int_{-\infty}^{\infty} dz' f(\theta;\xi',\eta',z')h(\xi-\xi',z-z',\eta')w(\eta')\end{aligned} \tag{22}$$

where $w(\eta)=1-\frac{\eta}{F}$ is the Jacobian factor.

The ideal projection data is

$$p(\theta,\xi,z)=\int_{-\infty}^{\infty} f(\theta;\xi,\eta,z)\frac{\sqrt{F^2+\xi^2}}{F}d\eta \tag{23}$$

Define a modified ideal projection data $p^m(\theta;\xi,\eta)$ as

$$p^m(\theta,\xi,\eta)=p(\theta,\xi,\eta)\frac{F}{\sqrt{F^2+\xi^2}}=\int_{-\infty}^{\infty} f(\theta,\xi,\eta,z)d\eta \tag{24}$$

where the FT of the ideal projection $p^m(\theta;\xi,\eta)$ is the same as eqn. (19), and the FT of fan-beam blurred data of eqn. (22) becomes

$$P^b(n,\omega_\xi,\omega_z)$$
$$= \int_0^{2\pi} d\theta\, e^{-2\pi i n\theta} \int_{-\infty}^{\infty} d\xi' e^{-2\pi i\omega_\xi \xi'} \int_{-\infty}^{\infty} dz' f(\theta;\xi',z,u) \qquad (25)$$
$$\times \int_{-\infty}^{\infty} d\xi\, e^{-2\pi i\omega_\xi \xi} \int_{-\infty}^{\infty} dz\, e^{-2\pi i\omega_z z} h(\xi,z,u) w(u(n,\omega_\xi,\xi'))$$

Therefore we will get

$$P^m(n,\omega_\xi,\omega_z) = P^b(n,\omega_\xi,\omega_z) H^{-1}(n,\omega_\xi,\omega_z)$$

where

$$H(n,\omega_\xi,\omega_z)$$
$$= \int_{-\infty}^{\infty} d\xi e^{-2\pi i\omega_\xi \xi} \int_{-\infty}^{\infty} dz e^{-2\pi i\omega_z z} h(\xi,z,u) w(u(n,\omega_\xi,\xi)) \qquad (26)$$

## IV. Filter for VFF Geometry

Using the geometric model for VFF geometry, the blurred projection data can be expressed, under the CCS, as

$$p^b(\theta,\xi,z) = \int_{-\infty}^{\infty} d\eta \int_{-\infty}^{\infty} dz^* \int_{-\infty}^{\infty} d\xi^* w(\xi^*,\eta) f(\theta,\eta,\xi^*,z^*) \qquad (27)$$
$$* g(\xi^*, \xi-\xi^*, z-z^*, \eta)$$

where w(s) is the Jacobian factor given by

$$w(\xi,\eta) = 1 - \frac{\eta}{F} + \frac{\eta\xi F'}{F^2} \qquad (28)$$

and g(.) is the PSF for VFF geometry.

Note that the collimator-blurred data is no longer a convolution of object with PSF, it also depends on the source position. Generally speaking, the integral of eqn. (27) cannot be separated to generate a filter as in the parallel-beam case.

A first simple consideration is to use an average PSF $\tilde{g}(.)$ to substitute g(.) in eqn. (27). Similar to the derivation in fan-beam geometry, after the 3D FT with respect to θ, ξ and z, it can be shown that

$$P^m(n,\omega_\xi,\omega_z) = P^b(n,\omega_\xi,\omega_z)\tilde{G}^{-1}(n,\omega_\xi,\omega_z) \qquad (29)$$

where $P^m(n,\omega_\xi,\omega_z)$ is 3D FT of the blur-free projection data, and $\tilde{G}$ is

$$\tilde{G}(n,\omega_\xi,\omega_z) = \int dz e^{-2\pi i\omega_z z} \int d\xi e^{-2\pi i\omega_\xi \xi} w[u(n,\omega_\xi,\omega_z,\xi,z)]$$
$$* \tilde{g}[u(n,\omega_\xi,\omega_z,\xi,z),\xi,z] \qquad (30)$$

Secondly, to better estimate $\tilde{g}(.)$, we note that the PSF is often a sharp function, i.e., only none-zero in a small region, and in this region, we can assume that the PSF does not change much. Therefore, eqn. (27) can be integrated in segments with $g = g_i(\xi-\xi', z-z', \eta)$ in each segment. With this approximation, the FT of eqn. (27) upon variable ξ will be

$$\int_{-\infty}^{\infty} d\xi\, e^{-2\pi i\omega\xi}\, g(\xi-\xi^*,\xi^*,z-z',\eta)$$
$$= \sum_i \int_{\xi_i}^{\xi_{i+1}} d\xi\, e^{-2\pi i\omega\xi}\, g_i(\xi-\xi^*,z-z',\eta)$$
$$= \sum_i \int_{\xi_i-\xi^*}^{\xi_{i+1}-\xi^*} d\xi\, e^{-2\pi i\omega\xi^*}\, g_i(\xi,z-z',\eta)$$
$$= \sum_i \int_{-\Delta}^{\Delta} d\xi\, e^{-2\pi i\omega\xi^*}\, g_i(\xi,z-z',\eta)$$
$$= \int_{-\infty}^{\infty} d\xi\, e^{-2\pi i\omega\xi^*} \sum_i g_i(\xi,z-z',\eta)$$
$$= \int_{-\infty}^{\infty} d\xi\, e^{-2\pi i\omega\xi^*}\, \tilde{g}(\xi,z-z',\eta) \qquad (31)$$

Usually, resolution enhancement by inverse *G*(..) will have a cost of noise increase. To control the noise in the process, one regularization approach is to use a Wiener filter, which can be expressed as

$$W_F(n,\omega_\xi,\omega_z) = \frac{|G(n,\omega_\xi,\omega_z)|}{|G(n,\omega_\xi,\omega_z)|^2 + \frac{N}{S}} \qquad (32)$$

where *N* is the expected value of the power spectrum of the noise process, and *S* is an estimate of the power spectrum of the random process of which the object is assumed to be a sample.

## V. Simulation Results

### A. 2D Filter Examples for Different Geometries

The presented Wiener filter of eqn. (32) for parallel-, fan- and VFF geometries are shown in Figure 4 in two dimensions. Multiplying it to the blurred sinogram gives the restored projections.

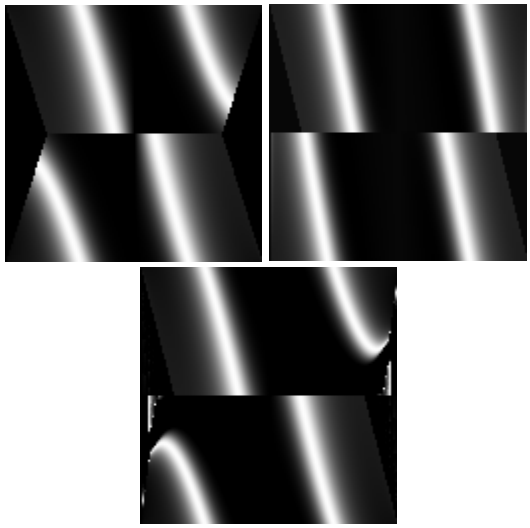

Fig. 4. Examples of 2D Wiener filter for inverse PSFs of parallel-beam (top left), fan-beam (top right), and VFF-beam (bottom) geometries, respectively.

### B. Phantom Experiments

Applying the VFF Wiener filter of eqn. (32) to the blurred projection data of the Shepp-Logan phantom, we obtained a noticeable improvement in the reconstructed images as illustrated in Figure 5.

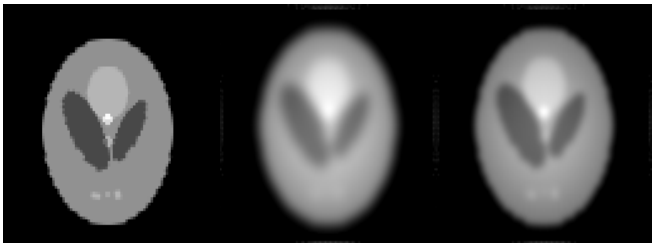

Fig. 5. VFF collimated SPECT studies, where $f(x)=a+b|x|$, $a$ = 60, and $b$ = 0.2. Left image is the Shepp-Logan phantom; the middle one is the reconstructed image without filtering; and the right is the result with filter applied before reconstruction.

## VI. Discussions And Conclusions

The filtering technique for non-parallel geometries is developed from their parallel counterpart. However the derivation itself is not strictly exact. Actually, from eqn. (25) to (26) we intentionally changed the variable $\xi$' to variable $\xi$ in order to separate the integrands for constructing the filter. This is a main challenging problem for this FDR-based method, in which an analytical explicit inversion filter does not exist, except for parallel-beam geometry. The reason is that for non-parallel geometries, the influence of any point at certain distance contributes not only to certain frequency $n$ and $\omega$, but also to the spatial variable $\xi$ as shown in eqns. (16) and (17). In another words, a simple "frequency to distance" relation no longer exists for non-parallel beam geometries! In general we are facing the following "convolution", instead of a simple frequency-domain filtering:

$$P_{ideal}(n,\xi,z) = \int ds\, P_{blur}(n,s) H(\xi,s;n,\omega_z) \qquad (33)$$

Usually a convolution method is not efficient as the filtering technique. But here it is a 1D integration, therefore, the computation time will not be a limiting factor. An accurate derivation and implementation of eqn. (33) for VVF collimators is currently under study.

In conclusion, we developed a filter for VFF geometry following the scheme used in parallel-, fan-, and cone beam SPECT. The FDR of VFF geometry and the shift variant GTF properties are derived. The averaged GTF is considered in the filter developing. We tested the method by the Shepp-Logan phantom using VFF collimator with a focal length function of $F=a+b|x|$. An improvement after compensation for the blurring effect is observed. The method is computationally efficient. It has the same limitation as the fan- and cone-beam collimators do [16]. Further research to remove this limitation for shift variant response correction is under progress.

## VII. References


[1] G. Han, *Image Reconstruction in Quantitative Cardiac SPECT with Varying Focal-length Fan-beam Collimators*, Ph.D. Dissertation, State University of New York at Stony Brook, NY, 2000.

[2] R. Novikov, "An Inversion Formula for the Attenuated X-ray Transformation", Preprint, May 2000.

[3] L. Kunyansky, "A New SPECT Reconstruction Algorithm Based on the Novikov's Explicit Inversion Formula", *Inverse Problems*, **17**: 293-306, 2001.

[4] H. Lu , J. Wen, X. Li, T. Li, G. Han, and Z. Liang, "Toward an Analytical Solution for 3D SPECT Reconstruction with Non-uniform Attenuation and Distance-dependent Resolution Variation: a Monte Carlo simulation study", *SPIE Med Imaging,* **4684**: 20-28, 2002.

[5] J. Wen, T. Li, X. Li, and Z. Liang, "Fan-beam and Variable Focal-length Fan-beam SPECT Reconstruction with Non-uniform Attenuation", *J. Nuclear Medicine Technology*, **30**: 97, 2002.

[6] J. Wen, T. Li and Z. Liang, "Ray-driven Analytical Fan-beam SPECT Reconstruction with Non-uniform Attenuation", *Proc. IEEE International Symposium on Biomedical Imaging*, pp. 629-632, 2002.

[7] C. E. Metz, F. B. Atkins and B. N. Beck, "The Geometric Transfer Function Component for Scintillation Camera Collimators with Straight Parallel holes", *Phys Med Biology,* **25**: 1059-1070, 1980.

[8] B. M. W. Tsui and G. T. Gullberg, "The Geometric Transfer Function for Cone and Fan Beam Collimators", *Phys. Med. Biology*, **35**: 81-93, 1990.

[9] G. L. Zeng and G. T. Gullberg, "Frequency Domain Implementation of the Three-Dimensional Geometric Point Response Correction in SPECT Imaging", *IEEE Trans. Nucl. Science*, **39**: 1444-1453, 1992.

[10] P. R. Edholm, R. M. Lewitt and B. Lindholm, "Novel Properties of the Fourier Decomposition of the Sinogram", *Proceedings of SPIE Intl Workshop Physics Eng Computerized Multidimensional Image Processing*, pp. 169-173, 1986.

[11] W. G. Hawkins, P. K. Leichner and N. Yang, "The Circular Harmonic Transform for SPECT Reconstruction and Boundary Conditions on the Fourier Transform of the Sinogram", *IEEE Trans. Med. Imaging,* **7**: 135-148, 1988.

[12] R. M. Lewitt, P. R. Edholm, and W. Xia, "Fourier Method for Correction of Depth-dependent Blurring", *SPIE Med Imaging III,* **1092**: 232-239, 1989.

[13] S. J. Glick, B. C. Penney, M. A. King, and C. L. Byrne, "Noniterative Compensation for the Distance-Dependent Detector Response and Photon Attenuation in SPECT Imaging", *IEEE Trans. Med. Imaging*, **13**: 363-374, 1994.

[14] W. Xia, R. M. Lewitt, and P. R. Edholm, "Fourier Correction for Spatially Variant Collimator Blurring in SPECT", *IEEE Trans. Med. Imaging*, **14**: 100-115, 1995.

[15] J. Ye and Z. Liang, "Depth-Dependent Resolution Deconvolution for Myocardial Perfusion SPECT with Non-Circular Scan Orbit", *J. Nuclear Medicine*, **35**: 190, 1994.

[16] Z. Cao and B. M. W. Tsui, "A Filtering Technique to Compensate for Detector Response in Converging-Beam SPECT Reconstruction", *Phys. Med. Biology*, **39**: 1281-1293, 1994.